TSPO Imaging in Glioblastoma Multiforme: A Direct Comparison Between ^{123}I-CLINDE SPECT, ^{18}F-FET PET, and Gadolinium-Enhanced MR Imaging

Per Jensen[1], Ling Feng[1], Ian Law[2], Claus Svarer[1], Gitte M. Knudsen[1], Jens D. Mikkelsen[1], Robin de Nijs[2], Vibeke A. Larsen[3], Agnete Dyssegaard[1], Gerda Thomsen[1], Walter Fischer[4], Denis Guilloteau[5], and Lars H. Pinborg[1,6]

[1]Neurobiology Research Unit, Rigshospitalet, Copenhagen, Denmark; [2]Department of Clinical Physiology, Nuclear Medicine, and PET, Rigshospitalet, Copenhagen, Denmark; [3]Department of Radiology, Rigshospitalet, Copenhagen, Denmark; [4]Department of Neurosurgery, Rigshospitalet, Copenhagen, Denmark; [5]Université François-Rabelais de Tours, INSERM U930 "Imaging and Brain," Tours, France; and [6]Epilepsy Clinic, Department of Neurology, Rigshospitalet, Copenhagen, Denmark

Here we compare translocator protein (TSPO) imaging using 6-chloro-2-(4′-^{123}I-iodophenyl)-3-(*N*,*N*-diethyl)-imidazo[1,2-a]pyridine-3-acetamide SPECT (^{123}I-CLINDE) and amino acid transport imaging using *O*-(2-^{18}F-fluoroethyl)-L-tyrosine PET (^{18}F-FET) and investigate whether ^{123}I-CLINDE is superior to ^{18}F-FET in predicting progression of glioblastoma multiforme (GBM) at follow-up. **Methods:** Three patients with World Health Organization grade IV GBM were scanned with ^{123}I-CLINDE SPECT, ^{18}F-FET PET, and gadolinium-enhanced MR imaging. Molecular imaging data were compared with follow-up gadolinium-enhanced MR images or contrast-enhanced CT scans. **Results:** The percentage overlap between volumes of interest (VOIs) of increased ^{18}F-FET uptake and ^{123}I-CLINDE binding was variable (12%–42%). The percentage overlap of MR imaging baseline VOIs was greater for ^{18}F-FET (79%–93%) than ^{123}I-CLINDE (15%–30%). In contrast, VOIs of increased contrast enhancement at follow-up compared with baseline overlapped to a greater extent with baseline ^{123}I-CLINDE VOIs than ^{18}F-FET VOIs (21% vs. 8% and 72% vs. 55%). **Conclusion:** Our preliminary results suggest that TSPO brain imaging in GBM may be a useful tool for predicting tumor progression at follow-up and may be less susceptible to changes in blood–brain barrier permeability than ^{18}F-FET. Larger studies are warranted to test the clinical potential of TSPO imaging in GBM, including presurgical planning and radiotherapy.

Key Words: neurooncology; SPECT; PET; MRI

J Nucl Med 2015; 56:1386–1390
DOI: 10.2967/jnumed.115.158998

Glioblastoma multiforme (GBM) remains the most common and aggressive primary tumor of the central nervous system. With conventional radiotherapy, chemotherapy, and debulking surgery, mean survival from diagnosis is 14.6 mo (*1*).

GBM lesions are strongly enhanced on contrast-enhanced structural imaging (CT or MR imaging), but populations of glioma cells are also present in the peritumoral environment. Thus, in clinical trials the volume for radiotherapy has been defined as the region of enhancement plus an isotropic margin of 2–3 cm (*1*). The combination of MR imaging and *O*-(2-^{18}F-fluoroethyl)-L-tyrosine PET (^{18}F-FET) improves the sensitivity and specificity of tumor tissue detection (*2*,*3*). However, ^{18}F-FET is not entirely glioma-specific, and increased uptake has been documented in astrogliosis secondary to infection, ischemia, radiation injury, demyelination, and hematoma (*4*–*7*). The 18-kDa translocator protein (TSPO) is a component of the mitochondrial permeability transition pore and is strongly expressed by glioma cell lines (*8*). In tissue resected from patients with astrocytoma, TSPO density correlates positively with malignancy and cell proliferation index and negatively with survival (*9*). 6-chloro-2-(4′-^{123}I-iodophenyl)-3-(*N*,*N*-diethyl)-imidazo[1,2-a]pyridine-3-acetamide SPECT (^{123}I-CLINDE; MAP Medical Technologies) has been validated as a second-generation TSPO tracer for use in humans (*10*) and recently in a GL26 mouse model of glioma (*11*). We present ^{123}I-CLINDE SPECT, ^{18}F-FET PET, and gadolinium-enhanced MR imaging results from 3 GBM patients at baseline compared with contrast-enhanced structural imaging at follow-up and hypothesize that ^{123}I-CLINDE SPECT at baseline is an imaging biomarker of GBM progression.

MATERIALS AND METHODS

The study was performed in accordance with the ethical standards of the Declaration of Helsinki and approved by the ethical committee of the Copenhagen Capital Region (approval H-2-2010-086, amendment 39319). All subjects signed an informed consent form. Three patients in an advanced state of GBM (World Health Organization grade IV) were included and genotyped for the rs6971 polymorphism to determine the TSPO binder status as described previously (*10*). Before inclusion, all patients had undergone surgery and received radiotherapy and chemotherapy with temozolomide, bevacizumab and irinotecan. In addition, patients 2 and 3 had been treated with a cell-based immunotherapy. Patient 2 had undergone surgical resection between baseline and follow-up MR imaging. The patients were scanned with ^{123}I-CLINDE, ^{18}F-FET, and MR imaging within 2 d. Patients 1 and 2 were rescanned with MR imaging after 6 and 17 wk, respectively, and patient 3 was rescanned with CT after 4 wk. The patients received no treatment with angiogenesis-inhibiting drugs for 6 wk before the scans and no radiochemotherapy between scans.

Received Apr. 8, 2015; revision accepted Jul. 6, 2015.
For correspondence or reprints contact: Lars H. Pinborg, Neurobiology Research Unit, Copenhagen University Hospital, Building 6931, Blegdamsvej 9, DK-2100 Copenhagen, Denmark.
E-mail: pinborg@nru.dk
Published online Jul. 16, 2015.

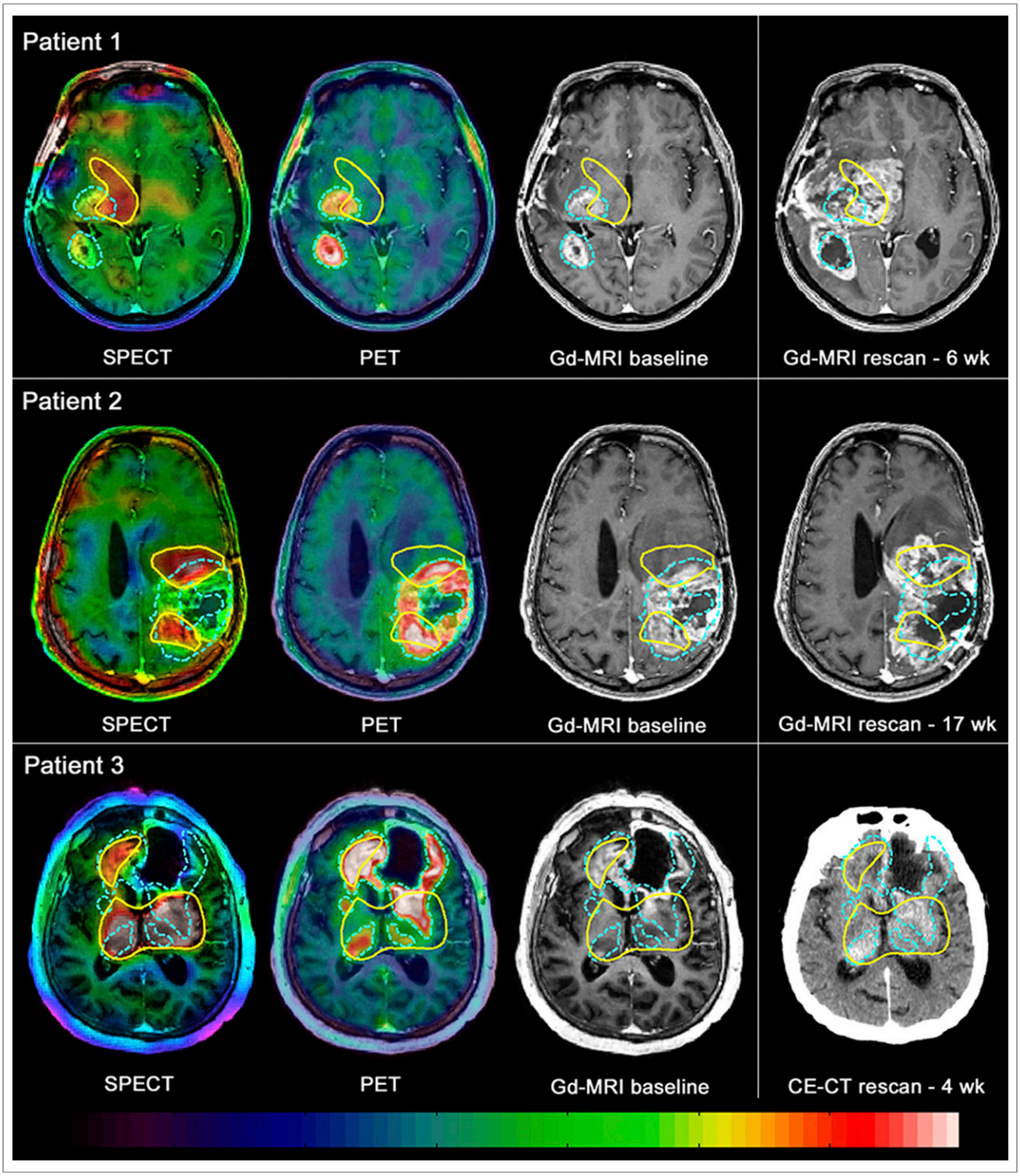

FIGURE 1. Weighted mean 0- to 150-min ^{123}I-CLINDE SPECT scans, summed 20- to 40-min ^{18}F-FET PET scans, and gadolinium- or contrast-enhanced (CE) structural scans at baseline and at rescanning. Blue VOIs show high ^{18}F-FET tumor uptake, and yellow VOIs high ^{123}I-CLINDE binding. Comparison of baseline and rescanning structural scans reveals that tumor expands predominantly in areas of high ^{123}I-CLINDE binding.

TABLE 1
Patients

Patient	Sex	Age (y)	Binder status	Rescanning modality	Interval (wk)	^{123}I-CLINDE injected dose (MBq)
1	F	48	MAB	MR imaging	6	191
2	M	65	LAB	MR imaging	17	188
3	M	64	MAB	CT	4	188

TABLE 2
VOIs

Patient	^{18}F-FET	^{123}I-CLINDE	^{18}F-FET ∩ ^{123}I-CLINDE	MR imaging (baseline)	MR imaging/CT (follow up − baseline)
1	17.3	36.6	2 (12%)	7.2	97.5
2	196.9	97.9	62.6 (32%)	150.5	NA
3	180	140.7	75 (42%)	60.7	44.8

NA = not applicable.
Data are in milliliters.

TABLE 3
Volumes in Common Between Baseline Structural Imaging and ^{123}I-CLINDE or ^{18}F-FET PET

Patient	^{18}F-FET (mL)	^{123}I-CLINDE (mL)	Sørensen–Dice coefficient between…	
			^{18}F-FET and MR imaging	^{123}I-CLINDE and MR imaging
1	6.7 (93%)	1.1 (15%)	0.54	0.05
2	120.1 (80%)	44.4 (30%)	0.69	0.36
3	48.0 (79%)	18.3 (30%)	0.4	0.18

TABLE 4
Volumes in Common Between Tumor Progression at Follow-up Structural Imaging and Baseline ^{18}F-FET PET or ^{123}I-CLINDE

Patient	^{18}F-FET (mL)	^{123}I-CLINDE (mL)
1	7.7 (8%)	20.9 (21%)
3	24.6 (55%)	32.3 (72%)

Patients

Patient data, genotype, rescan modality, scan–rescan time intervals, and injected ^{123}I-CLINDE dose are presented in Table 1.

Image Acquisition

After bolus injection of ^{123}I-CLINDE, dynamic SPECT images were acquired with a triple-head IRIX camera (Philips Medical) for 2.5 h as previously described (*10*), and weighted mean images were generated for region analysis.

A single-frame static PET acquisition was performed 20–40 min after intravenous injection of approximately 200 MBq of ^{18}F-FET on a 64-slice-CT Biograph TruePoint PET/CT scanner (Siemens). All PET scans were attenuation-corrected using low-dose CT performed immediately before the PET scan and were subsequently corrected for scatter and dead time. Images were reconstructed with an ordered-subsets expectation maximization 3-dimensional algorithm (6 iterations, 16 subsets) and a 5-mm gaussian filter. All patients fasted for at least 6 h before ^{18}F-FET injection.

T1-weighted MR imaging was performed on a 3-T MR Verio scanner (Siemens). Gadolinium was used in a dose of 0.1 mmol/kg of body weight (Multihance [Bracco] or Gadovist [Schering]). Patient 3 was rescanned using a CT scanner (Siemens) and a CT contrast agent containing 70 mL of iodine (350 mg/mL) (Omnipaque; GE Healthcare).

Data Processing

The weighted mean ^{123}I-CLINDE SPECT image was coregistered to the MR image of the same patient using interactive image overlay (*12*). ^{18}F-FET PET images and the follow-up MR images were coregistered to the first MR image of the same subject, applying the automatic rigid-body model included with Statistical Parametric Mapping, version 8 (*13*).

The definition of volumes of interest (VOIs) with high ^{123}I-CLINDE binding was standardized for all patients by automatically selecting voxels with a value above 1.5 times the mean cerebellar count. The delineation of high-uptake ^{18}F-FET volumes was standardized as previously described (*2*). A trained neuroradiologist supervised delineation of the MR imaging volumes. Baseline MR imaging VOIs were delineated manually as the contrast-enhanced areas of the coregistered baseline MR image. Blood vessels were omitted. Volumes for SPECT, PET, and MR imaging were determined, along with common volumes. Furthermore, the Sørensen–Dice coefficient for SPECT, PET, and baseline MR imaging was calculated as $\frac{2V_{A\cap B}}{V_A + V_B}$, with ∩ being the symbol of common volume. Volume of tumor progression was

defined as the additional contrast-enhanced volume from baseline to follow-up. For patient 2, follow-up volume analysis was not performed because of surgical resection between the baseline and follow-up scans.

RESULTS

Table 2 shows the sizes of the ^{18}F-FET and ^{123}I-CLINDE VOIs as well as the volumes in common for high-binding ^{123}I-CLINDE VOIs and high-uptake ^{18}F-FET VOIs. The VOIs of increased ^{123}I-CLINDE binding and ^{18}F-FET uptake showed varying degrees of overlap (12%–42%). Binder status does not appear to determine the volume of ^{123}I-CLINDE VOIs.

Table 3 shows the volumes in common between baseline structural imaging and ^{123}I-CLINDE or ^{18}F-FET PET. In all cases, baseline MR imaging VOIs showed greater similarity to ^{18}F-FET VOIs (Sørensen–Dice coefficients, 0.54, 0.69, and 0.40) than to ^{123}I-CLINDE VOIs (Sørensen–Dice coefficients, 0.05, 0.36, and 0.18). The percentage overlap of MR imaging baseline VOIs was greater for ^{18}F-FET VOIs (79%–93%) than for ^{123}I-CLINDE VOIs (15%–30%).

Table 4 shows the volumes in common between tumor progression at follow-up structural imaging and baseline ^{18}F-FET PET or ^{123}I-CLINDE. In the 2 patients for whom follow-up tumor progression volumes were estimated, the volume with de novo contrast enhancement at follow-up overlapped to a greater extent with ^{123}I-CLINDE VOIs than with ^{18}F-FET VOIs (21% vs. 8% and 72% vs. 55%).

DISCUSSION

This study follows 4 previous studies demonstrating TSPO in 1–3 patients with GBM using the TSPO PET tracer ^{11}C-PK11195 PET (*14–17*). To our knowledge, this is the first study to address the clinical value of TSPO imaging in GBM patients by comparing the second-generation TSPO SPECT tracer ^{123}I-CLINDE with ^{18}F-FET PET and contrast-enhanced structural imaging.

The first aim of the present study was to evaluate the similarity of ^{123}I-CLINDE and ^{18}F-FET VOIs. We found only limited VOI overlap, indicating that imaging of amino acid uptake and TSPO binding reflects different aspects of GBM pathology. Increased ^{18}F-FET uptake has been documented experimentally and clinically in reactive astrogliosis secondary to infection, ischemia, radiation injury, demyelination, and hematoma, indicating that ^{18}F-FET is not entirely glioma-specific (*4–7*). In contrast, no TSPO expression was found in reactive astrogliosis in a recent study in untreated human glioma patients (*17*). In addition to binding to glioma cells, TSPO tracers bind to myeloid cell lines, including glioma-associated microglia and macrophages (*18*). In contrast, uptake of ^{18}F-FET is not increased in areas of infiltrating activated macrophages and activated microglia in experimental abscesses (*4,19*). It may be hypothesized that TSPO-negative but ^{18}F-FET–positive areas represent primarily reactive astrocytosis, predicting a less aggressive development, but biopsy control confirmation is needed.

The second aim was to evaluate the correspondence between the VOIs of increased ^{18}F-FET uptake, the VOIs of increased ^{123}I-CLINDE binding, and volumes of MR imaging contrast enhancement at baseline. We found that ^{18}F-FET VOIs overlapped more (93%, 80%, 79%) with contrast-enhanced VOIs than with ^{123}I-CLINDE VOIs (15%, 30%, 30%). Contrast enhancement reflects a disturbed blood–brain barrier and could be related to treatment and tissue necrosis and not glioma cell proliferation per se (*20*). The binding of ^{123}I-CLINDE to TSPO does not appear to be significantly increased in areas of disrupted blood–brain barrier (*10*). It is known that glioma cells diffusely infiltrate brain tissue without disrupting the blood–brain barrier (*21*).

The third aim was to evaluate how ^{18}F-FET and ^{123}I-CLINDE VOIs overlap with VOIs representing tumor progression from baseline to follow-up on contrast-enhanced structural imaging. Follow-up VOI analysis was not performed for patient 2 because debulking surgery had taken place between baseline and follow-up scans and extravasation of gadolinium was highly increased in the area around the operation cavity on the follow-up scan. It appears that the VOIs of increased ^{123}I-CLINDE at baseline are a good visual predictor of tumor progression at follow-up (Fig. 1). In line with the visual interpretation, the percentage overlap with VOIs representing tumor progression is higher for ^{123}I-CLINDE than for ^{18}F-FET (21% vs. 8% and 72% vs. 55%) in patients 1 and 3. The findings correspond to previous reports demonstrating the contribution of TSPO to the uncontrolled cellular proliferation of glioma cells (*22*) and the correlation between TSPO density in surgically removed glioma tissue with clinical parameters such as survival time and tumor cell proliferation index (*8,9*). TSPO is expressed in glioma cells, suggesting that this method may be a more sensitive and specific marker of ongoing tumor cell proliferation and progression than conventional imaging methods. In addition, glioma-associated macrophages and monocytes contributing to tumor progression through the release of proinflammatory and proangiogenic factors may also add to the TSPO signal (*23*). Thus, the addition of TSPO imaging to^{18}F-FET PET has the potential to add information about areas of very active tumor cell proliferation in GBM. This may explain why low-grade gliomas have few or no TSPO binding sites (*17*).

CONCLUSION

These preliminary results from 3 patients with advanced GBM suggest that TSPO imaging is a sensitive and specific marker of GBM and that regional binding predicts areas of active tumor cell proliferation in GBM. Favorable implications can be foreseen for planning surgery and radiotherapy and monitoring the effect of oncologic therapy. ^{123}I-CLINDE SPECT appears to be less susceptible to blood–brain barrier disruption than ^{18}F-FET PET. However, to determine the exact role of TSPO imaging compared with imaging of amino acid transport, further studies are warranted.

DISCLOSURE

The costs of publication of this article were defrayed in part by the payment of page charges. Therefore, and solely to indicate this fact, this article is hereby marked "advertisement" in accordance with 18 USC section 1734. This work was financially supported by the European Union's Seventh Framework Programme (FP7/2007-2013), the Danish Council for Independent Research, the Research Committee of Rigshospitalet, and Desirée and Niels Yde's foundation. No other potential conflict of interest relevant to this article was reported.

ACKNOWLEDGMENTS

We acknowledge Svitlana Olsen and Melanie Ganz-Benjaminsen for technical assistance.

REFERENCES

1. Stupp R, Mason WP, van den Bent MJ, et al. Radiotherapy plus concomitant and adjuvant temozolomide for glioblastoma. *N Engl J Med.* 2005;352:987–996.
2. Pauleit D. O-(2-[^{18}F]fluoroethyl)-L-tyrosine PET combined with MRI improves the diagnostic assessment of cerebral gliomas. *Brain.* 2005;128:678–687.
3. Dunet V, Rossier C, Buck A, Stupp R, Prior JO. Performance of ^{18}F-fluoro-ethyl-tyrosine (^{18}F-FET) PET for the differential diagnosis of primary brain tumor: a systematic review and metaanalysis. *J Nucl Med.* 2012;53:207–214.
4. Salber D, Stoffels G, Pauleit D, et al. Differential uptake of O-(2-^{18}F-fluoroethyl)-L-tyrosine, L-^{3}H-methionine, and ^{3}H-deoxyglucose in brain abscesses. *J Nucl Med.* 2007;48:2056–2062.
5. Spaeth N, Wyss MT, Weber B, et al. Uptake of ^{18}F-fluorocholine, ^{18}F-fluoroethyl-L-tyrosine, and ^{18}F-FDG in acute cerebral radiation injury in the rat: implications for separation of radiation necrosis from tumor recurrence. *J Nucl Med.* 2004; 45:1931–1938.
6. Pichler R, Wurm G, Nussbaumer K, Kalev O, Silyé R, Weis S. Sarcoidosis and radiation-induced astrogliosis causes pitfalls in neuro-oncologic positron emission tomography imaging by O-(2-[^{18}F]fluoroethyl)-L-tyrosine. *J Clin Oncol.* 2010;28:e753–e755.
7. Floeth FW, Pauleit D, Sabel M, et al. ^{18}F-FET PET differentiation of ring-enhancing brain lesions. *J Nucl Med.* 2006;47:776–782.
8. Winkeler A, Boisgard R, Awde AR, et al. The translocator protein ligand [^{18}F] DPA-714 images glioma and activated microglia in vivo. *Eur J Nucl Med Mol Imaging.* 2012;39:811–823.
9. Miettinen H, Kononen J, Haapasalo H, et al. Expression of peripheral-type benzodiazepine receptor and diazepam binding inhibitor in human astrocytomas: relationship to cell proliferation. *Cancer Res.* 1995;55:2691–2695.
10. Feng L, Svarer C, Thomsen G, et al. In vivo quantification of cerebral translocator protein binding in humans using 6-chloro-2-(4′-^{123}I-iodophenyl)-3-(N,N-diethyl)-imidazo[1,2-a]pyridine-3-acetamide SPECT. *J Nucl Med.* 2014;55: 1966–1972.
11. Tsartsalis S, Dumas N, Tournier BB, et al. SPECT imaging of glioma with radioiodinated CLINDE: evidence from a mouse GL26 glioma model. *EJNMMI Res.* 2015;5:9.
12. Willendrup P, Pinborg LH, Hasselbalch SG, et al. Assessment of the precision in co-registration of structural MR images and PET images with localized binding. *Int Congr Ser.* 2004;1265:275–280.
13. Ashburner J, Friston K. Multimodal image coregistration and partitioning: a unified framework. *Neuroimage.* 1997;6:209–217.
14. Junck L, Olson JMM, Ciliax BJ, et al. PET imaging of human gliomas with ligands for the peripheral benzodiazepine binding site. *Ann Neurol.* 1989;26: 752–758.
15. Pappata S, Cornu P, Samson Y, et al. PET study of carbon-11-PK 11195 binding to peripheral type benzodiazepine sites in glioblastoma: a case report. *J Nucl Med.* 1991;32:1608–1610.
16. Su Z, Herholz K, Gerhard A, et al. [^{11}C]-(R)PK11195 tracer kinetics in the brain of glioma patients and a comparison of two referencing approaches. *Eur J Nucl Med Mol Imaging.* 2013;40:1406–1419.
17. Su Z, Roncaroli F, Durrenberger PF, et al. The 18-kDa mitochondrial translocator protein in human gliomas: an ^{11}C-(R)PK11195 PET imaging and neuropathology study. *J Nucl Med.* 2015;56:512–517.
18. Batarseh A, Papadopoulos V. Regulation of translocator protein 18 kDa (TSPO) expression in health and disease states. *Mol Cell Endocrinol.* 2010;327:1–12.
19. Kaim AH, Weber B, Kurrer MO, et al. ^{18}F-FDG and ^{18}F-FET uptake in experimental soft tissue infection. *Eur J Nucl Med Mol Imaging.* 2002;29: 648–654.
20. Brandsma D, van den Bent MJ. Pseudoprogression and pseudoresponse in the treatment of gliomas. *Curr Opin Neurol.* 2009;22:633–638.
21. Wen PY, Macdonald DR, Reardon DA, et al. Updated response assessment criteria for high-grade gliomas: response assessment in neuro-oncology working group. *J Clin Oncol.* 2010;28:1963–1972.
22. Austin CJD, Kahlert J, Kassiou M, Rendina LM. The translocator protein (TSPO): a novel target for cancer chemotherapy. *Int J Biochem Cell Biol.* 2013; 45:1212–1216.
23. Seyfried TN, Flores R, Poff AM, D'Agostino DP, Mukherjee P. Metabolic therapy: a new paradigm for managing malignant brain cancer. *Cancer Lett.* 2015; 356(2 Pt A):289–300.